

## ARTICLE TYPE

# Determination of wind-fed model parameters of High-Mass X-ray Binaries

Ali Taani,<sup>1</sup> Shigeyuki Karino,<sup>2</sup> Liming Song,<sup>3</sup> Chengmin Zhang,<sup>4</sup> and Sylvain Chaty<sup>4</sup><sup>1</sup>Physics Department, Faculty of Science, Al-Balqa Applied University, 19117 Salt, Jordan<sup>2</sup>Faculty of Science and Engineering, Kyushu Sangyo University, 2-3-1 Matsukadai, Higashi-ku, Fukuoka 813-8503, Japan<sup>3</sup>Key Laboratory of Particle Astrophysics, Institute of High Energy Physics, Chinese Academy of Sciences, Beijing 100049, China<sup>4</sup>National Astronomical Observatories, Chinese Academy of Sciences, Beijing 100012, China<sup>5</sup>School of Physics, University of Chinese Academy of Sciences, Beijing 100049, China

Author for correspondence: Ali Taani, Email: ali.taani@bau.edu.jo.

## Abstract

We have studied several neutron star high-mass X-ray binaries (HMXBs) with super-giant (SG) companions using a wind-fed binary model associated with the magnetic field. By using the concept of torque balance, the magnetic field parameter determines the mass accretion rate. This would help us to consider the relationship between wind velocity and mass-loss rate. These parameters significantly improve our understanding of the accretion mechanism. The wind velocity is critical in determining the X-ray features. This can be used to identify the ejection process and the stochastic variations in their accretion regimes. However, even in systems with a long orbital period, an accretion disk can be created when the wind velocity is slow. This will allow the HMXB of both types, SG and Be, to be better characterised by deriving accurate properties from these binaries. In addition, we have performed segmentation in the parameter space of donors intended for several SG-HMXB listed in our sample set. The parameter space can be categorised into five regimes, depending on the possibility of disk formation associated with accretion from the stellar wind. This can give a quantitative clarification of the observed variability and the properties of these objects. For most of the systems, we show that the derived system parameters are consistent with the assumption that the system is emitting X-rays through direct accretion. However, there are some sources (LMC X-4, Cen X-3 and OAO1657-415) that are not in the direct accretion regime, although they share similar donor parameters. This may indicate that these systems are transitioning from a normal wind accretion phase to partial RLOF regimes.

**Keywords:** keyword entry 1, keyword entry 2, keyword entry 3

## 1. INTRODUCTION

The detection of Cyclotron Resonance Scattering Features (CRSFs) in spectra of many accreting neutron stars (NSs) with high magnetic field ( $B \geq 10^{12}$  G) provides valuable insights into the physics of emitting regions and the evolution of these systems. They form due to resonant scattering processes with electrons, protons, and other ions in the plane and perpendicular to the magnetic field (Voges et al. 1982; Wilson et al. 2008; Ye et al. 2020). As a result, the cyclotron line features provide the only direct estimate of the magnetic field strength of NSs in X-ray binary systems. In High-Mass X-ray Binaries (HMXBs), a NS accretes matter from a companion star via stellar wind. The accreted matter is channeled along field lines of the strong magnetic field of the NS onto the magnetic poles. X-ray emission from the NS is produced in regions around the magnetic poles. It is noteworthy to mention here that most observed cyclotron lines have been detected above 10 keV and are interpreted as electron features, with inferred magnetic fields  $B \sim 10^{12}$  G (Heindl et al. 2001). The combined effects of poor statistics, photoelectric absorption and the lack of evidence for a remnant accretion disk have made these energy sources elusive.

Most efforts to calculate theoretical cyclotron lines have been performed in a line-forming region with a constant temperature and density of an electron-proton plasma permeated

by a uniform magnetic field (Wheaton et al. 1979; Orlandini et al. 1999; Yamamoto et al. 2011; Ye et al. 2019). Nishimura (2005) calculated cyclotron lines assuming a strong variation in field strength with distance from an emission region. However, no model generating such high flux and high temperature at a layer deeper than absorbing heavy atoms has been proposed.

According to recent studies, several pulsars show changes in luminosity dependence in the cyclotron resonance energy. The first aim of this paper is to derive magnetic field strengths, which is crucial for these systems, and obtain clues about the evolution of HMXBs, which can be understood in terms of the conservative evolution of normal massive binary systems.

The second aim of this study is to derive unknown parameters of HMXBs without uncertainty in the strength of the NS magnetic field. With robust data on the NS magnetic field, combined with spin period ( $P_{\text{spin}}$ ) and orbital period ( $P_{\text{orb}}$ ), we can fix several hitherto-unknown parameters, such as wind velocity and wind mass loss rate. These parameters influence significantly the model of wind-fed binary systems and can constrain the effects of binary evolution (Taani & Khasawneh 2017; Dai et al. 2017; Taani et al. 2019a,b; Karino et al. 2019; El Mellah et al. 2019a,b; Karino 2020). From this standpoint, with observations of NS magnetic fields, we could constrain the end products of HMXBs, such as a NS-NS merger, which is considered to be one of the most powerful gravitational

wave sources and also the most probable site for heavy element creation (Taani 2015; Postnov & Yungelson 20016; Haniewicz *et al.* 2020).

In the next section, we introduce the recent results of NS magnetic field given by CRSF observations. In Section 3, we discuss the method to obtain hitherto-unknown binary parameters from robust data on the NS magnetic field in SG-HMXBs. In Section 4, we discuss our findings. The last section is devoted to conclusions.

## 2. Cyclotron lines

Since the physical conditions are expected to vary over the emission region, the X-ray spectrum is expected to change with the viewing angle and therefore with pulse phase. This variation can be because during one rotation phase different parts of the surface are exposed and also due to change in local field structure due to accretion dynamics, e.g. change in accretion rate, as is seen for sources like Her X-1 and V0332+53. The difference in time scales of variation for  $E_{cyc}$  and luminosity will allow researchers to distinguish between these two distinct cases. (Nagase *et al.* 1991; Wilson *et al.* 2008). In this work, we have selected 11 persistent sources with SG companions known to have at least one cyclotron line (see Table 1). Here, our analysis of all pointing observations provides an opportunity to infer the values of magnetic field strength according to their spectra. However, the gravitational redshift  $z$  that at the NS surface is approximately

$$z \simeq \frac{1}{\sqrt{1 - \frac{2GM_{NS}}{R_{NS}c^2}}} - 1 \simeq 0.3 \quad (1)$$

where  $M_{NS}$ ,  $R_{NS}$  and  $c$  are the NS mass, radius and speed of light, respectively. Assuming canonical values for  $M_{NS}$  and  $R_{NS}$  of  $1.4 M_{\odot}$  and 10 km, thus  $z = 0.3$ . As such, the line energy of the fundamental cyclotron line is related to the magnetic field strength by the equation

$$E_{cyc} = 11.6B_{12}(1+z)^{-1}. \quad (2)$$

Here  $B_{12}$  is the magnetic field strength in units of  $10^{12}$  G, and the higher harmonics have an energy  $n$  times the fundamental energy  $E_{cyc}$ .

In general, the magnetic field of NSs spans a range from  $10^8$  G or less (LMXBs) to  $10^{15}$  G (magnetars); this concentration seems rather odd. Additionally, the magnetic field shows no correlation with the spin period of NSs and orbital period of the binary systems (see Fig. 1) This result disagrees with the dependence of B-field on the spin period in Be-systems shown by previous studies (Corbet 1986,2004; van den Heuvel 2009; Mardini *et al.* 2019a,b). Though, of course, we need to consider some observational biases: too strong of a magnetic field prevents accretion onto the NS and we could not observe such systems as bright X-ray sources (Taani 2016). Besides such possibility of biases, this concentration around  $B \approx 10^{12}$  G will draw a lot of interest and promote further studies on the NS magnetic field (Taani *et al.* 2019a,b). The fundamental energy covers a wide range, starting at 10 keV for Swift J1626.6-5156

(DeCesar *et al.* 2009) to 100 keV for LMC X-4 (La Barbera *et al.* 2001).

The strong energy variation of the cyclotron lines (for example, in V0332+53, GRO J1008-57 and GX301-2) can be used to argue that during different phases of the X-ray pulses, regions with different magnetic fields are observed.

It is noteworthy to mention here that 4U 0115+634 is one of the pulsars whose CRSFs have been studied in great detail (see, e.g., Wheaton *et al.* 1979; Nagase *et al.* 1991; Nishimura 2005). In previous outbursts, CRSFs have been detected up to the fifth harmonic (Heindl *et al.* 2003; Ferrigno *et al.* 2011). This high number of detected CRSFs in 4U 0115+634 makes this system an outstanding laboratory to study the physics of cyclotron lines in X-ray pulsars.

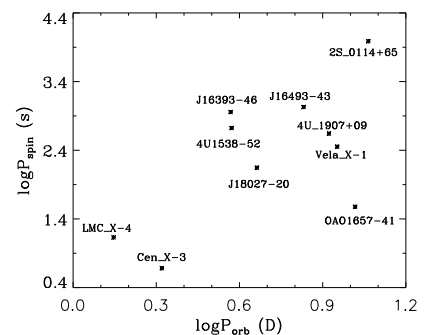


Figure 1. The Corbet diagram of SG-HMXBs.

**Table 1.** List of some observational parameters of all known persistent sources with supergiant companions through the cyclotron resonant scattering features

Object	$P_{\text{spin}}$ (s)	$P_{\text{orbit}}$ (d)	$E_{\text{cyc}}$ (keV)	Ref.
4U 1907+09	439	8.37	$18.8 \pm 0.4$	1, 2, 3
4U 1538–52	529	3.73	$21.4^{+0.9}_{-2.4}$	2, 4, 6, 5
Vela X-1	283	8.96	$27^{+0.5}_{-1.1}$	7, 8, 9, 10
Cen X-3	4.8	2.09	$30.4^{+0.3}_{-0.4}$	2, 8, 11
LMC X-4	13.5	1.4	$100 \pm 2.1$	8, 12
OA01657-415	37.7	10.4	36	13, 14, 15
J16493-4348†	1069	6.78	$33 \pm 4$	16, 17
4U 1700-377	–	3.4	37	15, 18
2S 0114+65	9700	11.6	22	19, 20
J16393-4643	904	4.2	$29.3^{+1.1}_{-1.3}$	21
IGR J18027-201	140	4.6	23	22

References.– These references are to period measurements in the literature. Some have errors originating from applied analysis, designated with a dagger, or from the supplied data, designated with an asterisk. (1) Cusumano et al. 1998; (2) Coburn et al. 2002; (3) Rivers et al. 2010; (4) Clark et al. 1990; (5) Rodes-Roca et al 2009; (6) Robba et al. 2001; (7) Kretschmar et al. 2005; (8) Makishima et al. 1999; (9) Kreykenbohm et al. 2002 (10) Schanne et al. 2007 (11) Santangelo et al. 1998; (12) Barbera et al. 2001; (13) Orlandini et al. 1999; (14) Denis et al. 2010; (15) Pottschmidt, S et al. 2011 (16) Nespoli et al. 2010 (17) D’Ai et al. 2011 (18) Reynolds et al. 1999 (19) Bonning et al. 2005 (20) denHartog et al. 2006 (21) Bodaghee et al. 2016. (22) Lutovinov et al. 2017.

### 3. Investigating wind parameters in SG HMXB systems

Under the assumption that the spin period of a NS is nearly in equilibrium, its magnetic field strength can be estimated by

$$B_{\text{NS}} = 2.184 \times 10^{12} \text{G} \times \left( \frac{M}{10^{18} \text{g s}^{-1}} \right)^{1/2} \left( \frac{P_s}{1 \text{s}} \right)^{7/6}, \quad (3)$$

assuming that the mass of the NS is  $1.4 M_{\odot}$  and its radius is 10 km (Ghosh & Lamb 1979; Campana et al. 2002; Tsygankov et al. 2016). The parameter  $\zeta$  is the ratio of accretion velocity to the free-fall velocity, and hereafter we fix this value as 0.5.

The mass accretion rate  $\dot{M}$  can be obtained as the following, if we assume the Hoyle-Lyttleton accretion scenario (Karino et al. 2019).

$$\dot{M} = \dot{m}_w \times \frac{G^2 M_{\text{NS}}^2}{a^2 v_w v_{\text{rel}}^3}, \quad (4)$$

where  $\dot{m}_w$  is the wind mass loss rate from the donor. Here, orbital radius  $a$  can be obtained from the orbital period of the system. The X-ray luminosity is related to the mass accretion rate as follows

$$L_X \simeq \frac{GM_{\text{NS}} \dot{M}}{R_{\text{NS}}}. \quad (5)$$

Thanks to this relation, we can deduce the mass accretion rate from the observed X-ray luminosity. The relative velocity of the wind to the NS is

$$v_{\text{rel}} = \left( v_{\text{orb}}^2 + v_w^2 \right)^{1/2} \quad (6)$$

and the velocity of the line-driven wind is usually prescribed in the model by so-called  $\beta$ -law .

$$v_w = v_{\infty} \left( 1 - \frac{R_d}{a} \right)^{\beta} \quad (7)$$

In this study, we assume  $\beta$ , which is a free input parameter, to be  $\beta = 1$  (Puls et al. 2008).  $v_{\infty}$  denotes the terminal velocity of the wind.

The wind parameters such as  $\dot{m}_w$  and  $v_{\infty}$  contain large uncertainties. Combining above equations with CRSF data

introduced in the previous section, however, a single relationship between  $\dot{m}_w$  and  $v_{\infty}$  could be obtained for the canonical NS parameters. From Eqs. (3) to (7), we get

$$v_w^2 = -v_{\text{orb}}^2 \pm \sqrt{\frac{GM_{\text{NS}}^2}{\pi a^2 \dot{M}} \dot{m}_w}. \quad (8)$$

If the luminosity of the NS is known, the mass accretion rate  $\dot{M}$  could be derived from Eq. (5).  $a$  is the orbital semi-major axis and it is obtained from the orbital period if the mass of the donor is known. In Table 2, we show the values of donor mass and donor radius, which has appeared in Eq. (7).

If we choose the mass loss rate from the donor  $\dot{m}_w$  as a fundamental variable, then Eq. (8) becomes a biquadratic equation and has four solutions. Two of them are physically nonsense, so we consider the other two solutions since they have a clear correlation between wind velocity and the mass loss rate of donors in SG-HMXBs. These solutions of the wind velocity are shown in Figs. 2 - 4 by solid curves, as functions of mass loss rate in SG-HMXBs. In these figures, the wind parameter given by the frequently used wind model by Vink, de Koter, & Lamers (2001) are shown at the same time. In Vink, de Koter, & Lamers (2001), the approximated wind mass loss rates from SG stars are given by the complex functions of mass, radius (escape velocity), luminosity (effective temperature) of SG stars. To derive the mass loss rate of the HMXB donors, we use the mass and radius data introduced in previous papers (Chaty et al. 2008; Cusumano et al. 2010; Rawls et al. 2011; Mason et al. 2012; Falanga et al. 2015; Reig et al. 2016). From these data, we derive the effective temperature and corresponding luminosity using approximated stellar evolution scheme. We compile Eqs. (1) to (30) in and find the evolution stage of each donors in SG-HMXBs listed in Table 2. Then, we derive the effective temperature at this evolutionary stage.

The wind parameters ( $v_{\infty}$  and  $\dot{m}_w$ ) we obtained are reported in Table 2. From these results, we could confirm that terminal velocities of the wind from donors in SG HMXBs are rather slow. In seven systems, the terminal velocities of donors dip from the typical wind velocity of galactic single SG stars ( $1,000 - 2,000 \text{ km s}^{-1}$ ). This result is consistent with

**Table 2.** List of derived parameters for SG HMXBs

name	$B_{\text{NS}} [10^{12}\text{G}]$	$M_{\text{d}} [M_{\odot}]$	$R_{\text{d}} [R_{\odot}]$	$\log(L_{\text{d}}/L_{\odot})$	$T_{\text{eff}} [10^4\text{K}]$	$\nu_{\infty} [10^7\text{cm s}^{-1}]$	$\dot{m}_{\text{w}} [10^{-8}M_{\odot}\text{s}^{-1}]$
LMC X-4	11.2	15.0	7.7	4.50	2.78	22.4	1.10
Cen X-3	3.4	22.1	12.6	4.92	2.77	21.3	5.37
J16393	3.3	20	13	4.82	2.57	9.96	37.2
4U1538	2.4	14.1	12.5	4.67	2.40	8.53	25.7
J18027	2.6	21	19	4.90	2.22	8.44	44.7
J16493	3.7	47	32	5.64	2.62	19.5	776
4U1907	2.1	27.8	22.1	5.21	2.47	9.01	166
Vela X-1	6	24.0	31.8	5.21	2.06	6.98	3.72
OAQ1657	4	14.3	24.8	4.72	1.76	6.10	22.9
2S0114	2.5	16	37	4.85	1.55	5.28	33.9

The data on mass and radius of NS are taken from (Falanga et al. 2015; Reig et al. 2016; Chaty et al. 2008; Rawls Reig et al. 2011; Cusumano et al.2010; Mason et al.2012) . The luminosity and effective temperature are computed by their approximated stellar evolution track given by Hurley et al. (2001). From these donor data, the terminal velocity of the wind and the wind mass loss rate from SG stars are derived by polynomial approximation given by Vink et al. (2001).

recent result given by Giménez-García et al. (2016) who argued that the stellar wind of donors in persistent HMXBs is systematically slow<sup>a</sup>. For instance, from recent observations, it is suggested that the wind velocity in persistent SG HMXBs, Vela X-1, is relatively slow ( $\nu_{\infty} = 700\text{km s}^{-1}$ ). In our samples, even for systems with higher  $\nu_{\infty}$ , the wind velocities at the NS positions are typically  $\nu_{\text{w}} \approx 500\text{km s}^{-1}$ , and still show very slow wind.

It is broadly considered that in wind-fed HMXBs, the wind matter is captured by the NS magnetic field at a certain radius, and transported onto the polar regions of the NS. In this process, around the polar region, the accretion column is formed and the potential energy of the accretion matter is converted into strong X-ray radiation.

However, it is believed that, when the NS (and consequently NS magnetic field lines) rotates rapidly, the accretion matter cannot fall onto the NS surface and in some conditions it could be expelled out (Pfahl et al. 2002; Podsiadlowski et al. 2004). This rotational inhibition of the accretion matter is called the propeller effect (see Reig & Zezas 2018). The propeller / accretion limit could be defined by three typical radii (accretion radius  $r_{\text{a}}$ , magnetic radius  $r_{\text{m}}$  and corotation radius  $r_{\text{co}}$ ). The propeller regime is defined when the accretion radius of the disk is larger than the magnetic radius. In contrast, in the supersonic inhibition regime, the magnetic radius is larger than the accretion radius and corotation radius, thus it rotates more slowly than inner regions of the disk.

The parameter space could divided into five accretion regimes based on their magnitude relation (Stella, White, & Rosner 1986; Bozzo, Falanga, & Stella 2008). That is, the parameter space can be categorized into

- (A) supersonic inhibition regime ( $r_{\text{m}} > r_{\text{a}}, r_{\text{co}}$ ),
- (B) subsonic inhibition regime ( $r_{\text{co}} > r_{\text{m}} > r_{\text{a}}$ ),
- (C) supersonic propeller regime ( $r_{\text{a}} > r_{\text{m}} > r_{\text{co}}$ ),

a. On the other hand, the wind velocity in SFXT systems seems very fast ( $\nu_{\infty} = 1,500\text{km s}^{-1}$ ).

- (D) subsonic propeller regime ( $r_{\text{co}}, r_{\text{a}} > r_{\text{m}}, \dot{M} < \dot{M}_{\text{c}}$ ),
- (E) direct accretion regime.

Here,  $\dot{M}_{\text{c}}$  denotes the critical limit where radiative cooling starts working (see Bozzo et al. 2008).

In figures shown below (Figs. 2 - 4), the different accretion regimes (A) to (E) are divided by dashed lines. The shaded region denotes the direct accretion regime such that only systems in this region can be observed as a persistent HMXB. The efficiency of the propeller depends weakly on the magnetic moment of the star (Ustyugova et al. 2006). Since if the angular velocity of the star is larger, then the efficiency of the propeller becomes higher (Tsygankov et al. 2016). In contrast, in the inhibition regime the accreting matter will be prevented by the magnetic gate due to being gravitationally focused toward the NS and thus the centrifugal gate also propels away material along the magnetospheric boundary of the NS (Bozzo et al. 2016). In addition, the subsonic propeller regime becomes clearer as the strength of the propeller increases. As the strength increases there is a sharp decrease in the accretion rate to the star. In these figures, the solid curves represent the theoretical relations between  $\dot{m}_{\text{w}}$  and  $\nu_{\text{w}}$  given by Eq. (8) with the CRSF data. We show that when these curves come into the direct accretion region (shaded region) created in the figures, the systems with corresponding parameters can lead to X-ray emission.

## 4. Discussion

### 4.1 Wind parameters

In Figures 2-4, we show the direct accretion region where the systems with corresponding parameters can emit strong X-rays. In the same figures, we plot the wind parameters given by the standard wind model combined with the stellar evolution track; furthermore we show the theoretical relations between the  $\dot{m}_{\text{w}}$  and  $\nu_{\text{w}}$  given by Eq. (8) with the CRSF data. The position of each source is based on the results reported in Table 2. In systems shown in Figures 2 and 3, these plots show good consistency: the plots are located in the direct accretion

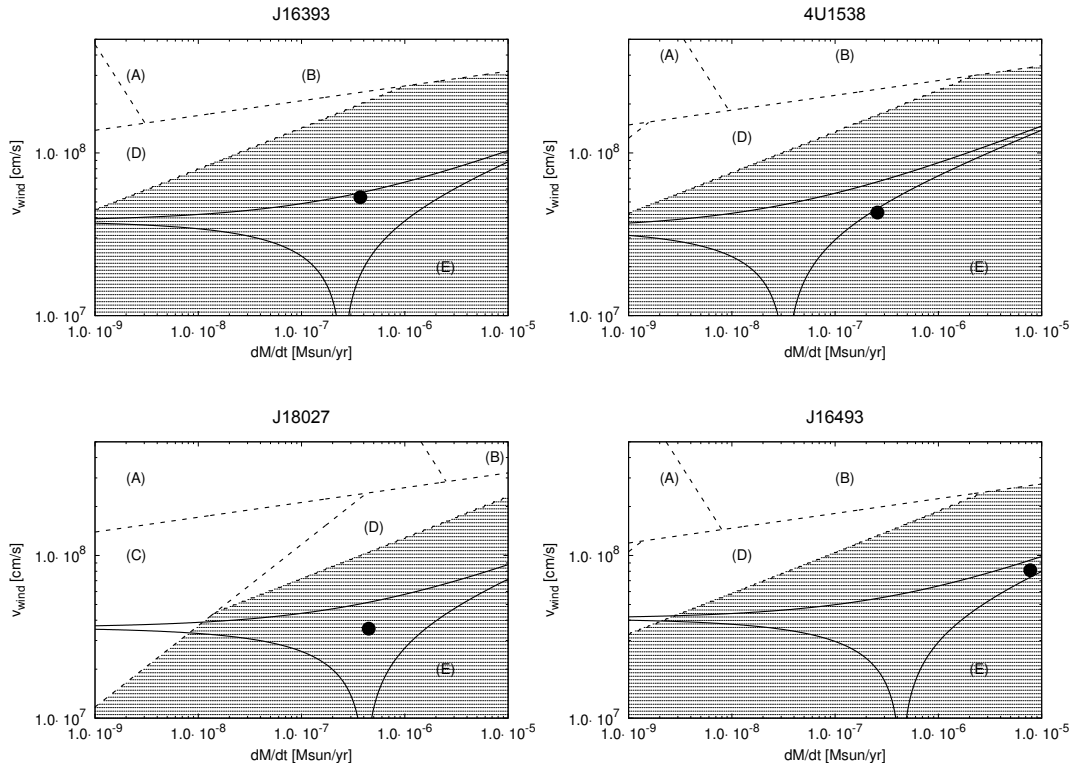


**Figure 2.** Plots of the wind velocity vs mass-loss rate, in various accretion regimes. The position of each source is shown by a black filled circle. As shown clearly, the parameter space can be categorized into (A) supersonic inhibition regime, (B) subsonic inhibition regime, (C) supersonic propeller regime, (D) subsonic propeller regime, and (E) direct accretion regime indicated by the shaded region, and the solution of the wind equation is represented by solid curves.

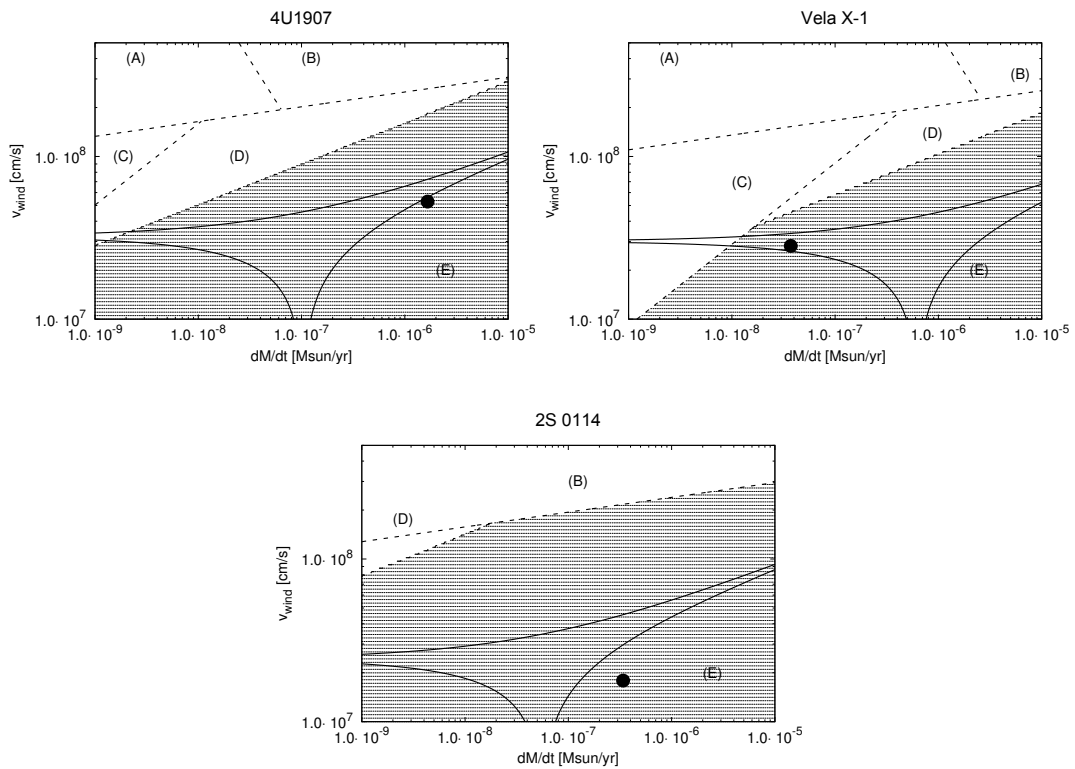


**Figure 3.** The same as previous, for the wind mass loss-rate, accretion mass-loss rate and accretion regimes. The position of each source is shown by a black filled circle.

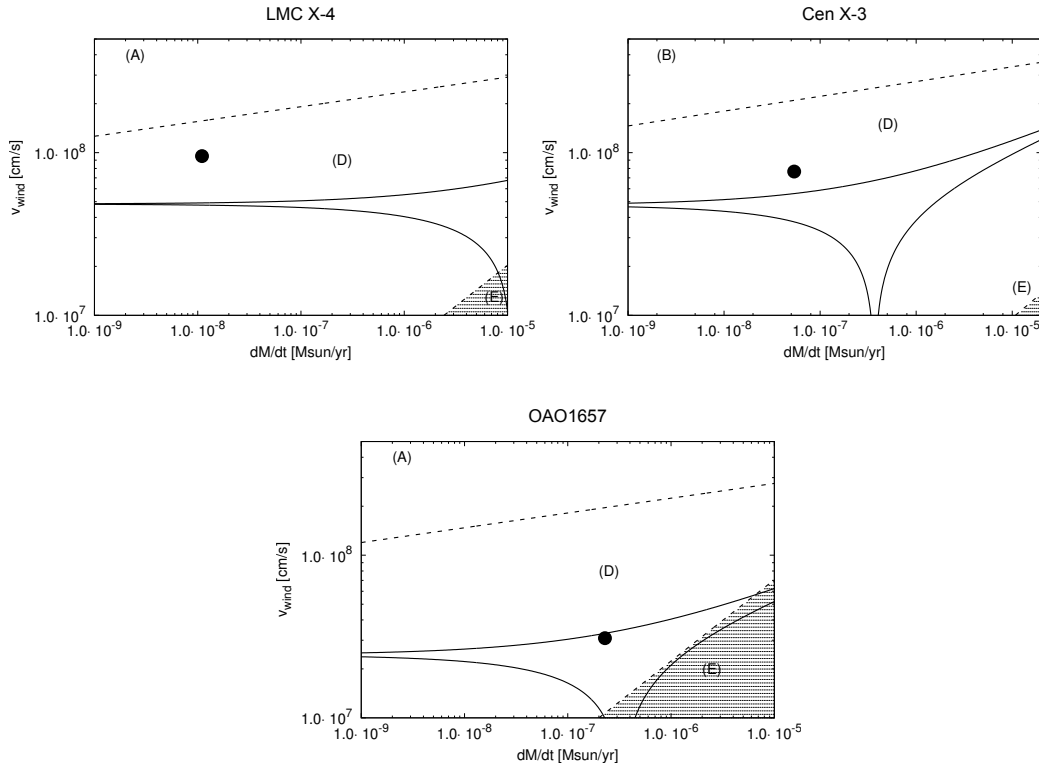


**Figure 4.** The same initial conditions in terms of the stellar wind parameters as in Figs. 2-3, but these sources show different features and different distributions.

region (shaded region) and roughly follow the theoretical curves (obtained with CRSF data). These result partly explain the slow wind tendencies in SG-HMXBs. Namely, when the wind velocity becomes too high, the wind plots might go outside of the accretion regime from the upper boundary of the shaded region. For typical mass loss rate in SG stars (say,  $10^{-7} M_{\odot} \text{yr}^{-1}$ ), the upper bound of the accretion regime is  $\approx 800 \text{km s}^{-1}$ . Then, the systems with fast-wind donors cannot be observed as bright persistent X-ray sources.

On the other hand, our model cannot be applied for three binaries, such as LMC X-4, Cen X-3 and OAO1657 (see Fig. 4) although they share similar donor parameters. Since in systems with shortest orbital periods (LMC X-4 and Cen X-3) the Roche-lobe filling factors approach quite near to 1, their accretion mode may not be typical wind accretion any more. Their accretion mode could enter in the regime of RLOF, or quasi RLOF (Shakura et al. 2012; Shakura et al. 2013). In this case, it is little wonder that we cannot obtain consistent wind parameters for these sources. Additionally, OAO1657 shows an inconsistent parameter set. As a result, the Roche lobe filling factor is much smaller and RLOF cannot be realized. On the other hand, it is suggested that the donor in this system is a Wolf-Rayet star (Mason et al. 2009; Mason et al. 2012). In this case, it might be ill-adapted to the standard wind model for typical SG stars. It is also argued that the system parameters of OAO1657 cannot be reproduced with standard binary evolution theory: a lot of mysteries remained in the understanding of this system (Jenke et al. 2012; Walter et al.

2015).

#### 4.2 NS magnetic field

The question of where exactly the magnetic field is measured still remains unanswered. This depends on the accretion geometry and flow and other mechanisms (Wei et al. 2010; Coburn et al. 2002; Kreykenbohm et al. 2005). Hence, their line profiles reflect the geometrical and physical properties of the accretion column near the magnetic poles of the NS, and therefore constitute a diagnostic tool for accessing the physics of accretion.

It is noteworthy to mention here that the NS magnetic fields in Table 2 are surprisingly concentrated in a narrow range  $\sim 10^{12} \text{G}$ . Despite the fact that their physical properties, in particular their energy band (10 - 100 keV) which govern the evolution, are different, they strongly depend on the assumed parameters, and these parameters dominate their evolutionary stages. Thus, the magnetic field itself is of fundamental significance to having a thorough insight into the physics of the emitting region structure, and could also be imperative to assisting us in improving our understanding of binary evolution. Otherwise, the implementation of known stellar evolution and observational statistics in population synthesis codes will remain a major issue in our understanding of the processes occurring in compact binaries or in the treatment of selection effects (Postnov & Yungelson 2006). However, our results shown in Figs. 2 - 4 clearly demonstrate the variety of SG-HMXBs based on the different types of interactions be-

tween the wind mass loss rate and the three NS radii (accretion radius, magnetic radius and corotation radius). This diversity of X-ray binary systems is important in principle, and could be used to demonstrate the properties of wind-fed systems such as SG-HMXBs, and the parameters entirely control their evolution, since the binaries with compact remnants are primary potential GW sources.

Finally, 1A 0114+650 is a unique source with unusual properties (very slow rotation period, relatively low X-ray luminosity and a super-orbital periodicity of 30.7 days (see Farrell et al., 2006)), exhibiting properties consistent with both Be and SG X-ray binaries (Walter et al. 2015). This source suggests that it evolves on a time scale of several years (Wang 2010), or may be an accreting magnetar candidate (Sanjurjo-Ferrin et al. 2017; Tong & Wang 2018). Possible signature of a transient disk was also found (Hu et al. 2017).

## 5. Summary and Conclusions

The following conclusions and implications are obtained:

We have determined new physical quantities for several HMXBs with supergiant companions through their cyclotron lines. These parameters are: the terminal velocity of the wind, mass-loss rate of the donor, magnetic field, effective temperature and corresponding luminosity. Furthermore, for all systems, our analysis (direct accretion condition shown by shaded region, and wind equation solution shown by solid curves) indicates that the wind velocity must be systematically slow.

By adopting the accretion regime model by Bozzo et al. (2008), we have explored the parameter space in several regimes to support the intrinsic variabilities of mass accretion rate and wind velocity. This may allow us to study an evolutionary path for several SG-HMXBs in these diagrams. Different regimes are sufficient to distinguish the bright X-ray sources spatially, and the magnetic field-wind velocity can be probed. As a result, persistent SG HMXBs within the shaded region can be observed through the direct accretion regime. This interpretation is predicated on its emission of accretion in high-energy X-rays.

It is seen that the wind velocity causes a significant effect on the results of their X-ray features and it could be used to determine the ejection mechanism. Consequently, when the wind velocity is slow, the accretion disk is often formed even in systems with large orbital period. This will allow to better characterize the HMXB of both types, SG and Be, hosting NS, by deriving accurate properties of those compact binaries.

From the updated measurement of HMXB cyclotron lines, the derived magnetic fields given by CRSF data are all concentrated around  $\sim 10^{12}$ G. However, the fundamental energy during X-ray observation, spin and other physical parameters property diverges and varies. The existence of a high magnetic field has the potential to regulate their formation and evolution.

The accretion mechanism for the fast spinning NSs ( $P_{spin} \leq 40$  s) with a short orbital period ( $P_{orb} \leq 10$  d), like in LMC X-4, Cen X-3 and OAO1657 (see Fig. 4) can not be con-

strained by our model. In LMC X-4 and Cen X-3, these two binary systems are extremely tight systems. Thus, the accretion mechanism can therefore not be approximated by spherical wind, because in such tight systems the concentrated asymmetric wind or RLOF accretion should be considered. Although OAO 1657 is a further evolved star with a long orbit, the donor of this system can be detected throughout its evolution as a Wolf-Rayet star with a stellar wind mass-loss rate.

Finally, we note that currently CRSFs data available are not sufficiently accurate or numerous to allow for precise analysis. One would hope that the results of this work will be improved with data from Suzaku, *INTEGRAL*, *eROSITA* and *HXMT*, which can provide significant increase in the observational sensitivity of a few cyclotron sources.

**acknowledgements:** We are grateful to A. D’Ai, E. Nespoli, O. Nishimura, M. Orlandini, K. Pottschmidt, R. Rothschild, V. Sguera, Gaurav Jaiswal, and S. Tsygankov, for their comments and suggestions that allowed us to improve the clarity of the original version. Special thanks to Nicola Masetti for comparing our data with the data in his web page <http://www.iasfbo.inaf.it>. A. Taani gratefully acknowledges support and hospitality from the Institute of High Energy Physics, Chinese Academy of Sciences through the CAS President’s International Fellowship Initiative (PIFI).

## DATA AVAILABILITY

The data that support the findings of this study are available from the corresponding author upon reasonable request.

## References

- [1] Bodaghee A, Tomsick J. A., Fornasini F. A. & et al. 2016, Accepted for publication in the ApJ, arXiv:1407.0112
- [Bondi & Hoyle(1944)] Bondi H. & Hoyle F., 1944, MNRAS, 104, 273
- [2] Bonning E. W., & Falanga M., 2005, A&A, 436, L31
- [3] Bozzo E., Falanga M. & Stella L., 2008, ApJ, 683, 1031
- [Campana et al.(2002)] Campana S., Stella L., Israel G. L. & et al., 2002, ApJ, 580, 389
- [Castor, Abbott & Klein(1975)] Castor J. I., Abbott D. C. & Klein R. I., 1975, ApJ, 195, 157
- [Chaty et al.(2008)] Chaty S., Rahoui F., Foellmi C. & et al., 2008, A & A, 484, 783
- [4] Clark G. W., Woo J. W., Nagase F. & et al. 1990, ApJ, 353, 274
- [5] Coburn W., Heind W. A., Rothschild R. E. & et al. 2002, ApJ, 580, 394
- [6] Coley J. B., Corbet R. H. D. & Krimm H. A., 2015, ApJ, 808, 140
- [7] Corbet R.H.D., 1986, MNRAS, 220, 1047

- [8] Corbet R.H.D., Coe M.J., Edge W.R.T. & et al. 2004, *Astron. Telegram*, 277, 1
- [9] Cusumano G., de Salvo T., Burderi L. & et al. 1998, *A&A*, 338, L79
- [Cusumano et al.(2010)] Cusumano G., La Parola V., Romano P. & et al., 2010, *MNRAS*, 406, 16
- [10] D’Ai A., Cusumano G., La Parola V. & et al. 2011, *A&A*, 532, A73
- [11] Dai Z.B., Szkody P., Taani A. & et al. 2017, *A&A*, 606, 45
- [12] DeCesar M. E., Pottschmidt K., & Wilms J., 2009, *ATel*, 2036
- [13] den Hartog P. R., Hermsen W., Kuiper L. & et al. 2006, *A&A*, 451, 587
- [14] Denis M., Bulik T. & Marcinkowski R., 2010, *AcA*, 60, 75D
- [15] El Mellah I., Sander A. A. C., Sundqvist J. O., & Keppens R., 2019a, *A&A*, 622, 189A
- [16] El Mellah I., Sundqvist J. O., & Keppens R., 2019b, *A&A*, 622, L3
- [Falanga et al.(2015)] Falanga M., Bozzo E., Lutovinov A., et al. 2015, *A&A*, 577, A130
- [17] Ferrigno C., Falanga M., Bozzo E. & et al. 2011, *A&A*, 532, 76A
- [18] Fürst F., Pottschmidt K., Wilms J. & et al., 2014, *ApJ*, 784, L40
- [19] Giménez-García A., Shenar T., Torrejón J. M. et al. 2016, *A&A*, 591A, 26G
- [Ghosh & Lamb(1979)] Ghosh P. & Lamb F. K., 1979, *ApJ*, 234,296
- [20] Heindl W. A., Coburn W., Gruber D. E. & et al. 2001, *ApJ* 563, L35
- [21] Heindl W. A., Coburn W., Kreykenbohm I. & et al. 2003, *ATel*, 200, 1
- [22] Hu C. P., Chou Y., Ng C. Y. & et al., 2017, *ApJ*, 844, 16
- [Hurley et al.(2000)] Hurley J. R., Pols O. R. & Tout C. A., 2000, *MNRAS*, 315, 543
- [23] Jenke P. A., Finger M. H., Wilson-Hodge C. A. & Camero-Arranz A., 2012, *ApJ* 759, 124
- [Karino & Miller(2016)] Karino S. & Miller J. C. , 2016, *MNRAS*, 462, 3476K
- [24] Karino S., Nakamura K.& Taani A., 2019, *Publications of the Astronomical Society of Japan*, 71, 58
- [25] Karino S., 2020, *Publications of the Astronomical Society of Japan* 72, 95
- [26] Kreykenbohm I., Coburn W., Wilms J. et al. 2002, *A&A*, 395, 129
- [27] Kreykenbohm I., Mowlavi N., Produit N. & et al. 2005, *A&A*, 433, 45
- [28] la Barbera A., Burderi L., Di Salvo T. & et al. 2001, *ApJ*, 553, 375
- [29] Lutovinov A. & Tsygankov S. 2017, *MNRAS*, 466
- [30] Makishima K., Mihara T., Nagase F. & et al. 1999, *ApJ*, 525, L97
- [31] Mardini M. K., Placco V. M., Taani A., & et al. 2019a, *ApJ*, 882, 27
- [32] Mardini M. K., Li H., Placco V. M., & et al., 2019b, *ApJ*, 875, 89
- [33] Mason A. B., Clark J. S., Norton A. J., et al. 2009, *A&A*, 505, 281
- [Mason et al.(2012)] Mason A. B., Clark J. S., Norton A. J.& et al., 2012, *MNRAS*, 422, 199
- [34] Nagase F., Dotani T., Tanaka Y. & et al. 1991, *ApJ*, 375, 49
- [35] Nespoli E., Fabregat J., & Mennickent R. E., 2010, *A&A*, 516, A106
- [36] Orlandini M., Dal Fiume D., Frontera F. & et al. 1999, *A&A* 349, L9
- [37] Pfahl E., Rappaport S., Podsiadlowski P. & et al. 2002, *ApJ*, 574, 364
- [38] Podsiadlowski P., Langer N., Poelarends A. J. T. & et al. 2004, *ApJ* 612, 1044
- [39] Postnov k. A. & Yungelson L. R., 2006, *Living Rev Relativ*, 9, 6
- [40] Pottschmidt K., Suchy S., Rivers E. & et al. 2011, *AIPC*, 1427, 60
- [41] Puls J., Vink J. S., & Najarro F., 2008, *A&A Rev.*, 16, 209
- [Rawls, Orosz & McClintock(2011)] Rawls M. L., Orosz J. A., McClintock J. E. & et al. 2011, *ApJ*, 730, 25
- [Reig, Nersesian & Zazas(2016)] Reig P., Nersesian A., Zezas A. & et al. 2016, *A&A*, 590, A122
- [42] Reig P., & Zezas A., 2018, *A&A*, 613A, 52R
- [43] Reynolds A. P., Owens A., Kaper L. & et al. 1999, *A&A*, 349, 873R
- [44] Rivers E., Markowitz A., Pottschmidt K. & et al. 2010, *ApJ*, 709, 179



- [45] Robba N. R., Burderi L., Di Salvo T. & et al. 2001, *ApJ*, 562, 950
- [46] Rodes-Roca J. J., Torrejón J. M., Kreykenbohm I. & et al. 2009, *A&A*, 508, 395
- [47] Sanjurjo-Ferrin G., Torrejon J. M., Postnov K., et al., 2017, *A&A*, 606, A145
- [48] Santangelo A., del Sordo S., Segreto A. & et al. 1998, *ApJ*, 340, 55
- [49] Sanwal D., Pavlov G., & Zavlin V. E., 2002, *ApJ*, 574, L61
- [50] Shakura N., Postnov K., Kochetkova A., & Hjalmarsdotter L., 2012, *MNRAS* 420, 216
- [51] Shakura N., Postnov K., & Hjalmarsdotter L., 2013, *MNRAS* 428, 670
- [Stella, White & Rosner(1986)] Stella, L., White, N. E. & Rosner, R., 1986, *ApJ*, 308, 669
- [52] Taani A., 2015, *Jordan Journal of Physics*, 8, 149
- [53] Taani A., 2016, *Research in Astronomy and Astrophysics*, 16, 101
- [54] Taani A. & Khasawneh A., 2017, *Journal of Physics: Conference Series*, 869, 012090
- [55] Taani A., Karino K., Song L. & et al. 2019a, *Journal of Physics: Conference Series* 1258, 012029
- [56] Taani A., Karino K., Song L. & et al. 2019b, *Research in Astronomy and Astrophysics*, 19, 12
- [57] Tong H. & Wang W., 2018, *arXiv:180605784T*
- [Tsygankov et al.(2016)] Tsygankov, S., Mushtukov, A. A., Suleimanov, V. F. & Poutanen, J., 2016, *MNRAS*, 457, 1101
- [58] Ustyugova G. V., Koldoba A. V., Romanova M. M. & et al. 2006, *ApJ*, 646, 304
- [59] van den Heuvel E. P. J. 2009, *Physics of Relativistic Objects in Compact Binaries: from Birth to Coalescence*, *Astrophysics and Space Science Library*, Jointly published with Canopus Publishing Limited, Bristol, UK, 359
- [Vink, de Koter & Lamers(2001)] Vink, J. S., de Koter, A. & Lamers, H. J. G. L. M., 2001, *A & A*, 369, 574
- [60] Voges W., Pietsch W., Reppin C. & et al., 1982, 263, 803
- [61] Walter R., Lutovinov A. & Bozzo E., 2015, *A&ARv*, 23, 2W
- [62] Wang W., 2010, *A&A*, 516, A15
- [63] Wheaton W., Doty J., Primini F. & et al. 1979, *Nature*, 282, 240
- [64] Wei Y. C., Taani A., Pan Y. Y. et al., 2010, *Chinese Physics Letters*, 27, 9801
- [65] Wilson C., Finger M. & Camero-Arranz A., 2008 *ApJ*, 678, 1263
- [66] Yamamoto T., Sugizaki M., Mihara T. & et al. 2011, *PASJ*, 63, 751
- [67] Ye C.Q., Wang D.H., Zhang C.M. & et al. 2019, *Astrophys. Space Sci.* 83, 230
- [68] Ye C.Q., Wang D.H., Zhang C.M. & et al. 2020, *Astrophys. Space Sci.* 365, 126